Tautomeric Self-Dimerization and Molecular Recognition Properties of 2-Aminopyrimidinone Derivatives as Triple Hydrogen-Bonding Modules in Molecular Assemblies

Hajime Abe,[a] Masayoshi Takase,[a] Yasuhiro Doi,[a] Shinya Matsumoto,[b] Masaru Furusyo,[c] and Masahiko Inouye*[a,d]

Dedicated to the memory of our teacher, Prof. Masaru Matsuoka, deceased January, 2002

Keywords: Molecular recognition / Self-assembly / Nucleobases / Hydrogen bonds / Tautomerism

A triple hydrogen-bonding module based on 6-alkynyl-2-amino-3*H*-pyrimidin-4-one was developed such as for self-dimerization and for nucleobase recognition processes. The strength of the module for the self-dimerization was determined by NMR and fluorimetric analyses in chloroform (ΔG_{298} = –22 to –23 kJ/mol). DFT calculations and X-ray structure analysis showed that the self-dimerization consists of the three-point hydrogen-bonding including two kinds of tautomers of the module in an ADD·DAA mode. Selective recognition of the module for a cytidine derivative was also observed, and the free energy change for the complexation (ΔG_{298} = –31 kJ/mol) is one of the highest values among triple hydrogen-bonded complexes so far reported.

Introduction

Because hydrogen bonding is a vectorial and easily tunable noncovalent interaction, the hydrogen bonds play a leading role in creating self-assembled molecular architectures.[1–3] Multiple hydrogen-bonding arrays composed of plural hydrogen-bond acceptor (A) and donor (D) groups have been widely used for such purposes taking advantage of homo- and heterodimerization characteristics of the arrays. In the simplest example, double hydrogen-bonding modules self-dimerized in a manner of an AD·DA pattern such as dimers of carboxylic acids, while quadruple hydrogen-bonding modules exhibited ADAD·DADA and AADD·DDAA ones.[3] Although the former is easily incorporated into the molecular structures, the relatively low binding energy of the double hydrogen bonding lacks general requirements for building strong and well-defined assemblies. While the latter, quadruple ones produce much stronger self-dimerized complexes, the limitation for the synthetic versatilities of them may offset the advantages. On the other hand, triple hydrogen bondings are seen in many natural environments, especially in double-helical DNAs, so that their information for the binding as well as their resources will readily be available. Of course, homodimerization is intrinsically impossible for the triple hydrogen-bonding modules because of the odd number with respect to the hydrogen-bonding units. We thought that this contradictory issue may be overcome by use of tautomerism of an ADD-type molecule to an AAD one; thus, an ADD·DAA triple hydrogen-bonding pattern could be constructed from a single molecular component.

Isocytosines, as representative 2-aminopyrimidin-4-ones have been known to exist as a mixture of their tautomers. The composition of the tautomers depends not only on the nature of media but also on the presence of hydrogen-bonding substrates. Conventionally, the tautomerism was studied mainly based on two kinds of the N–H tautomers, 2-amino-3*H*-pyrimidin-4-one (ADD type) and 2-amino-1*H*-pyrimidin-4-one (AAD type). As the tautomers show different absorption bands, the changes of the ratio were monitored by UV/Vis spectroscopy[4,5] and by magnetic circular dichroism.[4] In an EtOH solution, isocytosine mainly exists as the 3*H*-tautomer form, and in an aqueous solution, the equilibrium with the 1*H*-tautomer takes place.[4] The interaction

[a] Faculty of Pharmaceutical Sciences, Toyama Medical and Pharmaceutical University,
Toyama 930-0194, Japan
Fax: +81-76-434-5049
E-mail: inouye@ms.toyama-mpu.ac.jp
[b] Faculty of Education and Human Sciences, Yokohama National University,
Yokohama 240-8501, Japan
[c] Analysis Technology Research Center, Sumitomo Electric Industries Ltd.,
Itami 664-0016, Japan
[d] PRESTO, Japan Science and Technology Agency (JST), Japan

Supporting information for this article is available on the WWW under http://www.eurjoc.org or from the author.

for isocytosine with creatinine (AAD type) increased the ratio of the 3*H*-tautomer.[5] The dimeric forms (ADD·DAA) of isocytosine between the two tautomers were confirmed in crystalline[6,7] and co-crystalline states.[8] It was also reported that ADD·DAA-type self-dimerization of isocytosine was mediated by H^+ in crystal[6a,9] or ESI conditions.[10] Recently, in argon matrices or in gas phase, isocytosine was shown to exist predominantly as 2-aminopyrimidin-4-ol (ADA or ADD-type tautomer according to the geometry of OH bond) accompanied with a small part of the 3*H*-tautomer on the basis of its vibrational analyses,[11] and this observation was supported by theoretical analyses.[11–13] However, no systematic and comprehensive investigations on 2-aminopyrimidin-4-one derivatives as hydrogen-bonding modules were carried out especially in solutions. Thus, the full potential of their triple hydrogen-bonding motifs for self-dimerization processes remains elusive as it does in many other examples. Here we report tautomeric self-dimerization of 2-aminopyrimidin-4-one derivatives as well as their molecular recognition abilities for nucleobases in detail.

Results and Discussion

Molecular Design of Basic Skeletons

The solubility of the molecules that possess multiple hydrogen-bonding arrays is inherently poor in less polar solvents since the molecules can interact with each other through the hydrogen bonds to exist as network polymers of high molecular weight. Thus, improvement of their solubilities is essential not only for accurately assessing the intermolecular interactions in their "discrete" states but also for conducting their synthetic operations. To add solubility in less polar solvents but not to interfere with the hydrogen-bonding abilities, a long acyl or alkyl chain was introduced at 2-amino groups on 2-aminopyrimidin-4-ones. To the carbon-6 of the aminopyrimidinone ring, were linked alkynyl substituents that can modify the basicity of the hydrogen-bonding sites and act as a versatile linker for applying the aminopyrimidinones as a hydrogen-bonding module in complexed molecular assemblies (Figure 1). The latter reason will be documented in terms that ethynyl groups can easily be connected to a variety of aromatic and vinylic compounds by palladium-catalyzed cross-coupling reactions (see also below).

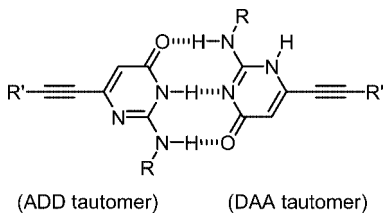

Figure 1. A tautomeric dimerization through an ADD·DAA-type triple hydrogen-bonding of 2-amino-3*H*-pyrimidin-4-one (left) and 2-amino-1*H*-pyrimidin-4-one (right) tautomers.

N-Acyl-2-amino-3*H*-pyrimidin-4-one Derivatives 3

As a starting point for this project, we chose *N*-acyl-2-amino-3*H*-pyrimidin-4-one as a self-dimerization module. Commercially available 2-amino-4-chloro-6-hydroxypyrimidine (**1**) was converted to *N*-octanoyl derivative **2**, which was alkynylated with tri-*n*-butyl(trimethylsilylethynyl)stannane by Stille coupling to give the desired compound **3** (Scheme 1). The spectroscopic properties such as ^{1}H and ^{13}C NMR and mass spectra of **3** were in agreement with the assigned structure. The solubility of compound **3** was found to be enough for permitting its binding examinations in less polar solvents such as $CHCl_3$ and CH_2Cl_2.

For the self- and cross-associations of **3**, **7**, and **9** (see below), the tautomerism of the monomer (e.g. between ADD, AAD, ADA, and DAD) may participate before the dimerization, and the dimer thus formed may also exist in tautomerism between three- and two-point hydrogen-bonded complexes (e.g. between A*AD*·*DA*A, *AAD*·*DDA*, and *AD*D·D*DA*; the hydrogen-bonded parts are in italics). Practically, it was impossible to evaluate each equilibrium constant for those possible tautomeric systems precisely. Thus, in the following discussion, "formal association constants" K'_{dim} and K'_a, obtained from the curve-fitting analyses for the plotting curves involving the influences of the tautomeric systems, were used for the evaluation of the strength of self- and cross-association. In the present study, fortunately, most of the plotting curves obtained fitted well into the theoretical curves assuming simple dimerization or 1:1 complexation.

The self-association tendency of **3** was first tested by plotting the relations of the ^{1}H NMR chemical shifts of the N*H*(*exo*) against the concentration of **3** in $CDCl_3$ (Figure S1, Supporting Information). However, the formal association constant was unexpectedly low ($K'_{dim} = 13 \pm 6$ M^{-1}). Cross-association of **3** (as an ADD-type molecule) was also studied with the lipophilic cytidine derivative **10C** (as a DAA-type molecule, Scheme 2). When 1 equiv. of **10C** was added to a 1.0×10^{-3} M $CDCl_3$ solution of **3**, the ^{1}H NMR signals of the N*H* protons were slightly shifted downfield by 0.11, 0.34, and 0.20 ppm for N*H*(*endo*), N*H*(*exo*) of **3**, and NH_2 of **10C**, respectively, indicating the presence of complementary triple hydrogen bonds (Figure 2). Quantitative assessment for the binding was carried out under the conditions in which the influence of self-association of not only **3** but also **10C** is relatively small. The 1:1 stoichiometry was confirmed by Job's plots for the chemical shift of N*H*(*exo*) protons of **3** (Figure S2, Supporting Information). The formal association constant (K'_a) for the cross-association was $1.11 \pm 0.02 \times 10^2$ M^{-1}, calculated by using an iterative curve-fitting analysis of the chemical shifts of N*H*(*exo*) for **3** in ^{1}H NMR titration (Figure S3, Supporting Information). As free energy changes (ΔG) can be calculated from association constants using $\Delta G = -RT\ln K_a$, the binding of **3** and **10C** yielded a stabilization energy ($-\Delta G_{295}$) of 11.6 kJ/mol. Systematic comparison of experimental $-\Delta G$ has been investigated, in which the values of ca. 20–30 kJ/mol were reported for the complexation by the amide–

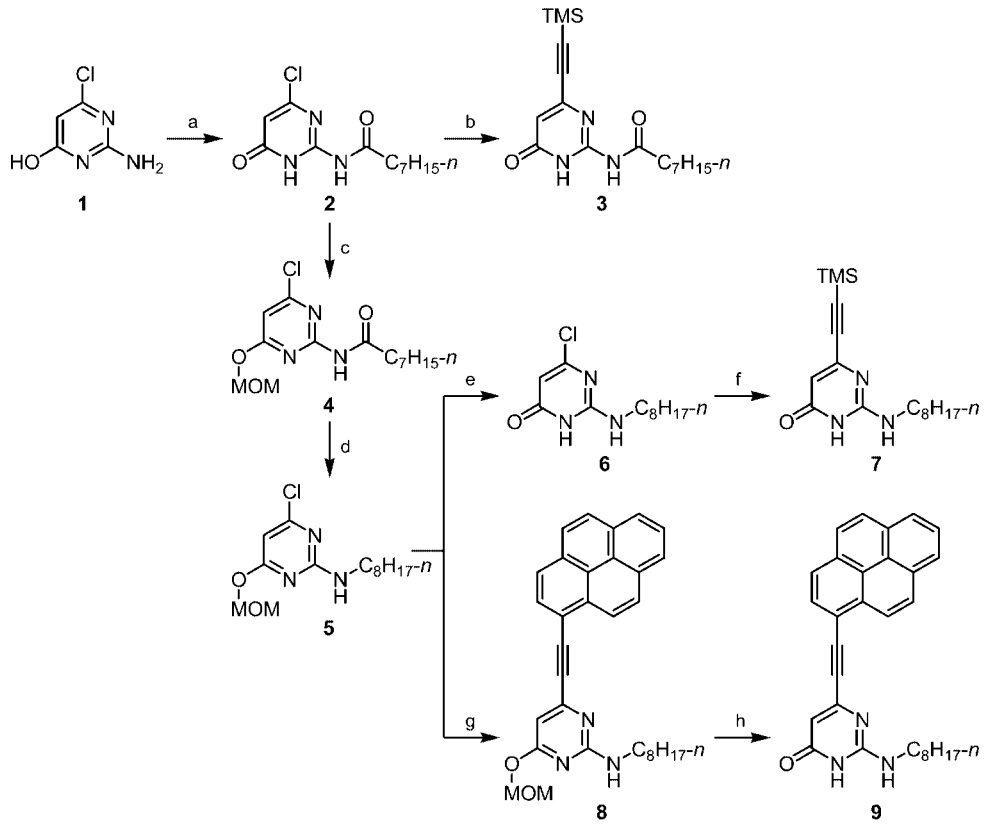

Scheme 1. Synthesis of **3**, **7**, and **9**; key: (a) *n*-octanoyl chloride, DMAP, DMF, 0 °C to room temp., 5 h, 77%; (b) [Pd(PPh$_3$)$_4$], tri-*n*-butyl(trimethylsilylethynyl)stannane, toluene, 80 °C, 5 h, 81%; (c) NaH, K_2CO_3, DMF, 0 °C, 1 h, then MOMCl, 0 °C to room temp., 24 h, 87%; (d) $LiAlH_4$, THF, reflux, 1 h, 56%; (e) aq. HCl, THF, room temp., 1 h, 100%; (f) [Pd(PPh$_3$)$_4$], tri-*n*-butyl(trimethylsilylethynyl)-stannane, xylene, 120 °C, 3 h, 22%; (g) 1-ethynylpyrene, [Pd(PPh$_3$)$_4$], Et_3N, THF, 60 °C, 12 h, 54%; (h) aq. HCl, THF, room temp., 1 h, 94%.

amide-type ADD·DAA triple hydrogen bonds.[1] Thus, the $-\Delta G$ value obtained for **3** and **10C** was significantly small compared to those for the previously exploited pairs having the same triple hydrogen-bonding pattern.

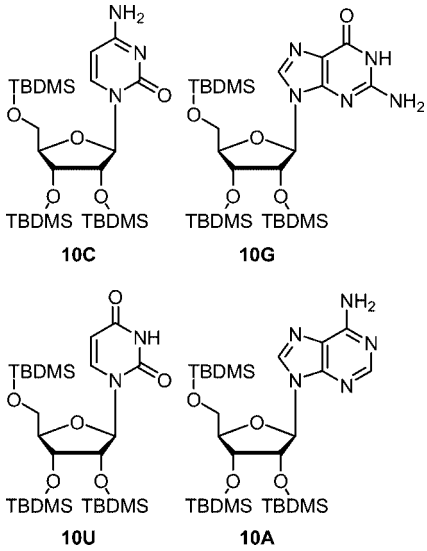

Scheme 2. Lipophilic nucleosides.

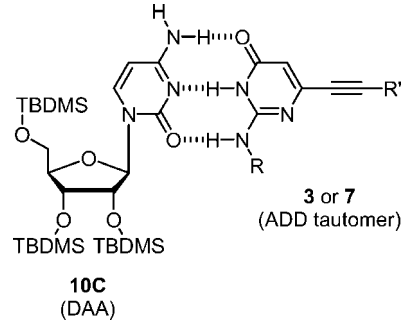

Figure 2. A possible complementary triple hydrogen-bonding recognition mode between **3** or **7** (ADD tautomer) and the cytidine derivative **10C** (DAA).

The reason for the low self- and cross-association abilities of **3** was searched through its stable conformations by quantum chemical calculations. B3LYP level hybrid density functional theory (DFT) and 6-31G(d,p) basis sets were applied for geometry optimizations and vibrational frequency analysis for using zero point energy (ZPE) correction. For simplification of the calculations, ethynyl and acetyl groups were substituted for (trimethylsilyl)ethynyl and *n*-octanoyl groups of **3**, respectively. The relative energies calculated for eight tautomeric and conformational isomers **3a**–**h** were

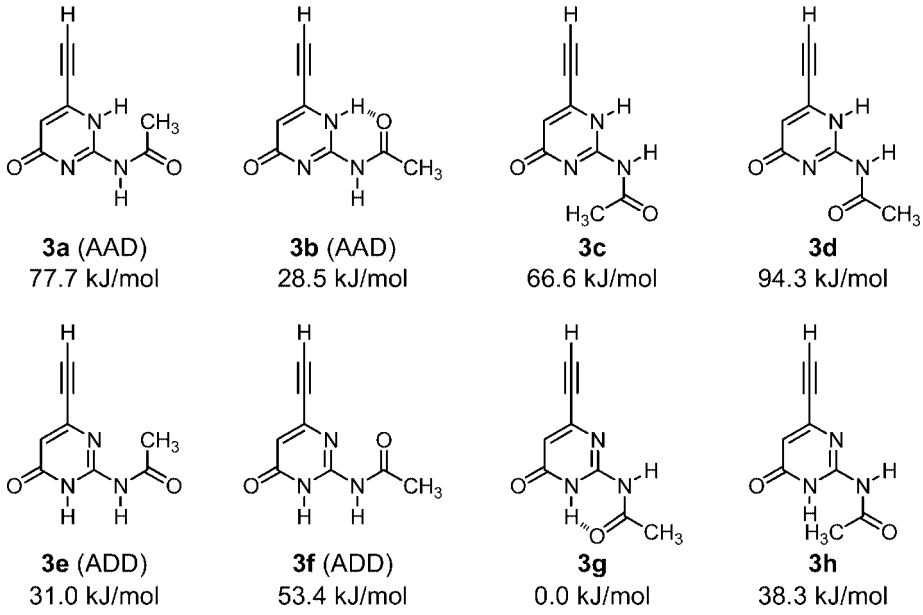

Scheme 3. Calculated relative stabilities of isomers **3a**–**h**; some substituents in **3** were simplified (see text); positive values indicated the degree of the instabilities from the most stable isomer **3g**; the hydrogen-bonding mode is shown in the parentheses.

shown in Scheme 3, in which positive values indicated the degree of the instabilities from the most stable isomer **3g**. The six-membered intramolecular hydrogen bonding may stabilize the conformation in **3g**, while the desired **3e** or **3f** as an ADD partner rather yields the electrostatic repulsion between the lone electron pairs of the pyrimidinone-1*N* and the *exo*-methyl or *exo*-amide-*O*. When **3** self-dimerizes in an ADD·DAA manner between **3e**,**f** and **3b**, the loss in the energy would arise resulting from the rotation about the pyrimidinone–amide axis in **3g** and also from the tautomerism of **3g** to **3b**. The energy loss might be too large to be compensated by the newly developed triple hydrogen-bonding interaction. In the case of the cross-association to the cytidine derivative **10C**, the same matter occurred to result in the observed weak interaction.[14]

Self-Dimerization of *N*-Alkyl-2-amino-3*H*-pyrimidin-4-one Derivatives 7 and 9

For suppression of the intramolecular hydrogen bond in **3**, the carbonyl groups of the *exo*-amide should be reduced to methylene groups. Thus, we newly designed *N*-alkyl-2-amino-3*H*-pyrimidin-4-one as a self-dimerization module. After MOM-protection of **2** to **4**, *N*-octanoyl group was reduced with $LiAlH_4$ to yield amine **5**. Acidic deprotection produced an *N*-alkyl parent skeleton **6**, which was alkynylated to **7** by Stille coupling. On the other hand, chloro substituent on **5** was replaced with 1-pyrenylethynyl group using Sonogashira reaction to afford **8**, followed by MOM-deprotection to a fluorescent module **9** (Scheme 1). As expected in "Molecular Design of Basic Skeletons" chapter (described above), the alkynyl function on the carbon-6 was found to be a versatile building block for constructing further sophisticated modules, and this technique can successfully be applied for using these modules to incorporate into self-assembling units.

^{1}H NMR dilution experiments of **7** in $CDCl_3$ at 22 °C revealed that at $\leq 4.0\times10^{-3}$ M, the signals of the N*H* and NCH_2 protons gradually shifted upfield with decreasing the concentration (Figure S4A, Supporting Information). A vapor pressure osmometry (VPO) analysis of **7** showed the apparent molecular weight as 625 g/mol at the concentration range from 2.5×10^{-3} to 2.5×10^{-2} M, suggesting the dimer formation of **7** (M_w = 319.5 g/mol). The formal association constant for the self-dimerization (K'_{dim}) was calculated by a curve-fitting method for the ^{1}H NMR chemical shifts of the NCH_2 protons, assuming that all the self-associated complexes exist as a dimer (Figure S4B, Supporting Information). The K'_{dim} value was $6.5\pm0.3\times10^3$ M^{-1}, which gives ΔG_{295} as –22 kJ/mol.

The strong self-dimerization abilities of *N*-alkyl-2-aminopyrimidinone derivatives were also studied by using UV/Vis and fluorescence spectroscopy. We investigated the relations of the absorbances (in the cases of **7** and **9**) and fluorescence emission intensities (in the case of **9**) upon their concentrations, respectively. At a lower concentration of the substrate, the absorbance fits in proportion to the concentration, obeying Beer's law. If deviation is observed from the linearity over a certain concentration, it means that self-interaction through the corresponding electron orbital becomes significant between two ground state molecules. Thus, the contribution of the intermolecular π-interaction (π-stacking) of **7** can be ruled out for its self-dimerization process, since the absorbance of **7** at both 250 and 325 nm obeyed Beer's law at the concentration range from 1.0×10^{-5} to 2.0×10^{-3} M in $CHCl_3$ (Figure S5, Supporting Information). Although no change for the shape of the absorption spectra was observed during the dilution at that con-

centration range, the self-dimerization of **7** was surely confirmed on the basis of the ^{1}H NMR dilution experiments (see above). The shape of the absorption spectra for **9** also showed no change at the concentration range from 5.0×10^{-6} to 2.0×10^{-4} M in $CHCl_3$ (data not shown). These findings indicate that π-stacking interactions are not important for the self-dimerization process in **7** and **9**. On the other hand, fluorescence spectra are much sensitive to the changes for the electronic nature of the substrates such as in the cases for hydrogen bonds. The fluorescence spectra of **9** were measured in $CHCl_3$ under various concentrations. The relative emission intensities at 450 nm well fitted into the theoretical curve calculated for the self-dimerization ($K'_{dim} = 1.1\pm0.2\times10^4$ M^{-1}) (Figure S6, Supporting Information), and the corresponding ΔG_{298} for **9** was –23 kJ/mol, which was close to that for **7** obtained on the basis of the NMR analysis. Noteworthy is that these values of K'_{dim} and ΔG are comparable to the reported ones for ADD·DAA-type heterodimeric complexes.[1] Fluorescence lifetime for **9** was also measured at 1.0×10^{-5} M, in which the monomer form predominates. The fluorescence decay curve of **9** (Figure S7, Supporting Information) was due to a one-component system in $CHCl_3$ ($\tau = 1.97\pm0.01$ ns), i.e., the pyrenyl module **9** showed only one kind of emission from the monomer form.

^{1}H NMR, UV/Vis, and fluorescence data of **7** and **9** implied that these *N*-alkyl-2-amino-3*H*-pyrimidin-4-one derivatives exist as a dimeric form over a certain concentration in less polar solvents through the triple hydrogen-bonding interactions. The dimerization mode of the pyrimidinones, however, remained to be clarified. Again quantum chemical calculations were used for solving this question in a manner similar to those conducted for *N*-acyl ones. In the present case, ethynyl and ethyl groups were substituted for (trimethylsilyl)ethynyl and *n*-octyl groups of **7**, respectively. For the tautomeric and conformational isomers **7a**–**f**, we calculated the relative energies by use of DFT(B3LYP) method and 6-31G(d,p) basis sets. In Scheme 4, the relative stabilities of the seven isomers were shown. Among the isomers, the 2-

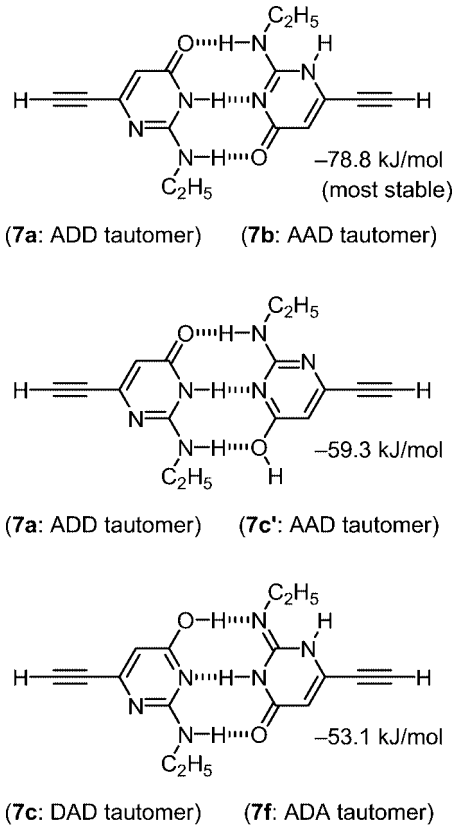

Scheme 5. The representative structures and their calculated relative stabilities of self-dimerized complexes of **7**; some substituents in **7** were simplified (see text); negative values indicated the degree of the stabilities from the double of the total energy of monomeric **7c**.

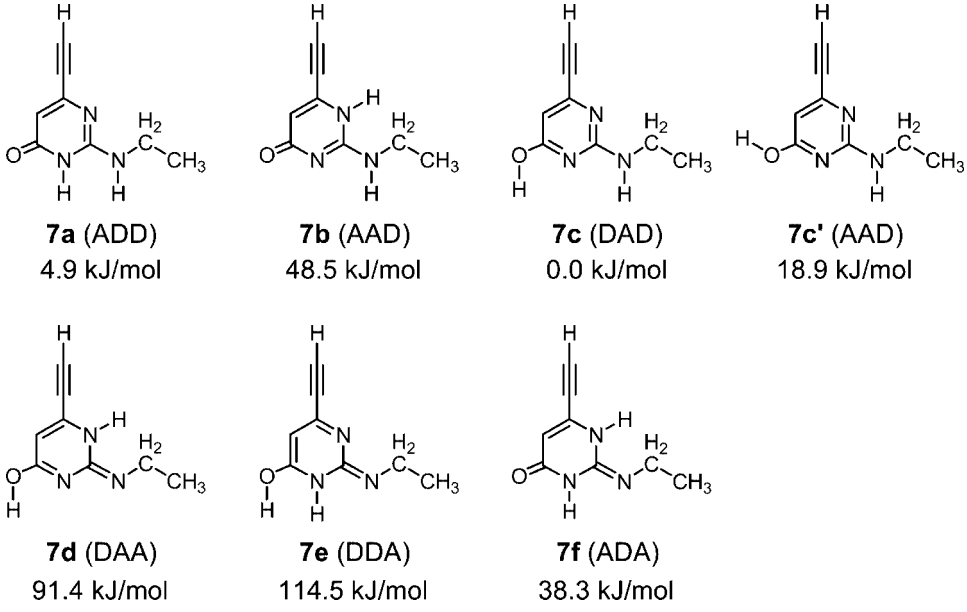

Scheme 4. Calculated relative stabilities of isomers **7a**–**f**; some substituents in **7** were simplified (see text); positive values indicated the degree of the instabilities from the most stable isomer **7c**; the hydrogen-bonding mode is shown in the parentheses.

aminopyrimidin-4-ol **7c** (DAD type) was predicted to be most stable in accordance with the reported calculations for isocytosine.[12,13] The calculation indicated that its conformational isomer **7c′** (AAD) was slightly less stable than **7c** by 18.9 kJ/mol, probably because of loss of the weak intramolecular hydrogen-bonding between the hydroxy O*H* and the pyrimidine-3*N*.

Some of possible dimerized structures for **7** were subjected to similar calculations. Three reasonable dimers **7a·7b**, **7a·7c′**, and **7c·7f** were studied as shown in Scheme 5, while the monomer components of **7d**,**e** were omitted because of their relatively high instabilities. Among the three, unexpectedly, the ADD·DAA pair **7a·7b**, which includes the less stable isomer **7b**, was predicted to be most stable. The DAD·ADA-type dimer **7c·7f** would be disadvantageous because of repulsive secondary interactions.[1,15] The difference between the two ADD·DAA dimers, **7a·7b** and **7a·7c′**, would be due to the difference in hydrogen-accepting abilities of the oxygen functionalities on **7b** and **7c′**: the former is carbonyl and the latter is hydroxy groups.[16] Thus, at least from the calculations, the self-dimerization mode in **7** was supposed as **7a·7b** form depicted in Scheme 5 (top).

Crystal Structure Analysis of *N*-Alkyl-2-amino-3*H*-pyrimidin-4-one Derivative 7

To evaluate the mode of this self-dimerization, determination of the crystal structure of **7** was tried by X-ray analysis. Slow evaporation of a $CDCl_3$ solution of **7** gave wet single crystals. Unfortunately, crystal data of good quality have not been attained to distinguish their isomers because of the disorder of terminal trimethylsilyl and octyl groups. Nevertheless, the obtained structure showed the notable intermolecular interactions between two molecules of **7** (Figure 3). They form complementary triple hydrogen-bonding in an exact 1:1 ratio, which consists of two kinds of its tautomers perhaps in an ADD·DAA mode as seen in the literature.[6,8,9]

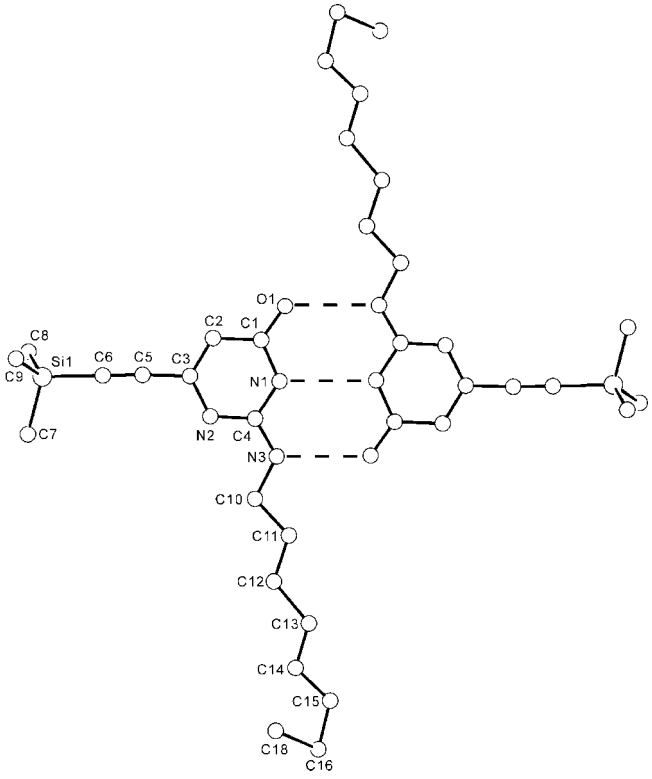

Figure 3. Crystal structure of **7**; intermolecular triple hydrogen-bonds are displayed as broken lines; hydrogen atoms are omitted; the molecules are only depicted in one of the two disordered conformations; for details, see Experimental Section.

Nucleobase Recognition Abilities of *N*-Alkyl-2-amino-3*H*-pyrimidin-4-one Derivatives 7 and 9

The molecular recognition abilities of the *N*-alkyl-2-aminopyrimidin-4-ones with nucleobases were investigated by ^{1}H NMR spectroscopy. When 1 equiv. of the cytidine derivative **10C** was added to a $CDCl_3$ solution of **7** (1.0×10^{-3} M), several characteristic changes were observed in their spectra. Both the signals for the N*H* protons of *endo*-amide and *exo*-amino groups on **7** were largely shifted downfield by 2.25 and 2.67 ppm, respectively. Although the signal for one proton of amino groups on **10C** was also shifted downfield from 5.04 to 9.36 ppm, that for the other amino proton shifted slightly upfield to 4.96 ppm in contrast (Figure 4). These phenomena will be explained by the formation of a complementary triple hydrogen-bonding interaction between **7** and **10C** as shown in Figure 2.[17] In the case of **10C** alone, the two amino protons are not distinguishable in the ^{1}H NMR spectrum because the 4-amino substituent rotates freely around the cytosine ring faster than the NMR time scale (part C in Figure 4). Generally, hydrogen bonds tend to fix the covalent bonds participated in the hydrogen-bonding against the rotation. Thus, when **10C** bound to **7**, the two amino protons on **10C** were no longer identical and appeared at different chemical shifts. Another notable point was that N–CH_2 protons in **7** showed splits after the association with **10C**, indicating the formation of a chiral complex between the chiral **10C** and the achiral **7**. However, the strong recognition ability of **7** to **10C** and self-association tendency of **7** did interfere with quantitative experiments for determining the association constants by use of NMR spectroscopy.

The fluorescence emission spectra of **9** changed upon the addition of **10C** in $CHCl_3$ under rather diluted conditions required for assessing the association constant ($\leq 1.0 \times 10^{-5}$ M). When **10C** was added incrementally to a $CHCl_3$ solution of **9** (1.0×10^{-6} M), two new emission bands appeared at λ_{max} = 414, 433 nm (Figure 5). There are isoemmisive points during this titration, which suggest the predominance of only two kinds of fluorescent species in the mixture, i.e., the monomer **9** and the complex **9·10C**. The analyses for the complexation were performed by measuring changes of the emission intensities at 410 nm. The 1:1 ratio of **9** and **10C** in the complex was confirmed by Job's plot (Figure S8, Supporting Information). The K'_a value was calculated to be $3.1 \pm 0.1 \times 10^5$ M^{-1} by a curve-fitting

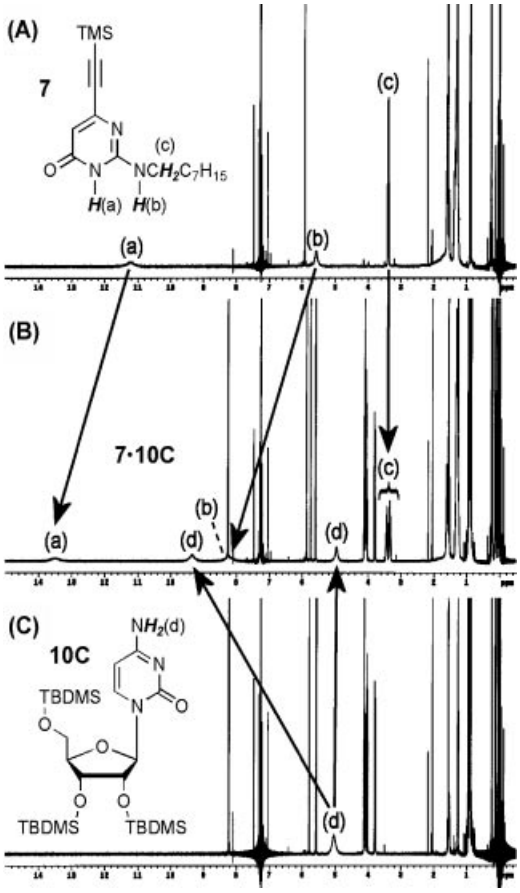

Figure 4. ^{1}H NMR (500 MHz) spectra of (A) **7**, (B) **7**·**10C**, and (C) **10C** in $CDCl_3$; conditions: **7** (1.0×10^{-3} M), **10C** (1.0×10^{-3} M), 22 °C; the signal (b) in (B) was assigned by the correlation with NCH_2 protons on COSY analyses.

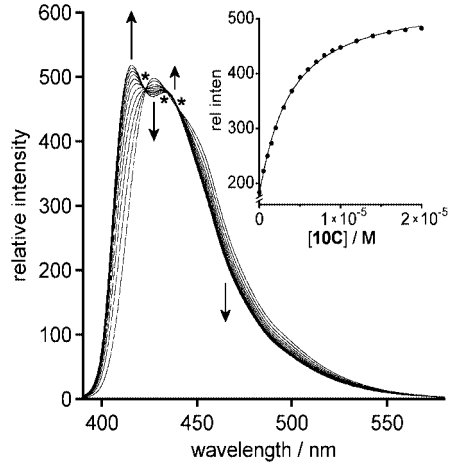

Figure 5. Fluorescent titration of **9** with **10C**; conditions: **9** (1.0×10^{-6} M), **10C** (0 to 10 equiv.), λ_{ex} = 375 nm, $CHCl_3$, 25 °C; inset shows the curve-fitting analysis based on the relative intensity at 410 nm; asterisks are marked on the isoemissive points.

method. Thus, the change in free energy for the complexation (ΔG_{298} = –31 kJ/mol) is one of the highest values among reported ones in artificial ADD·DAA-type hydrogen-bonding modules,[1] naturally occurring cytosine–guanine base pairs,[18] and their derivatives.[19]

These *N*-alkyl-2-amino-3*H*-pyrimidin-4-one modules were also found to have high selectivities to cytosine compared to other kinds of nucleobases. The affinities of **7** and **9** were surveyed using lipophilic nucleosides **10G**, **10A**, and **10U** (Scheme 2) on the basis of ^{1}H NMR and fluorescence analyses. When 1 equiv. of these nucleosides were added to a $CDCl_3$ solution of **7** (1.0×10^{-3} M), only small downfields of the chemical shifts of all the N*H* protons were observed, compared to the cases for **10C**. The results were summarized in Table 1. Furthermore, in the fluorescent titration of **9**, no meaningful changes were observed upon the addition of a large excess of **10G**, **10A**, and **10U**. This nucleobase selectivity of the modules for cytosine is interesting, and possibly is due to the relative stability of the ADD structure among its tautomers, being supported by quantum chemical calculations (see Supporting Information).

Conclusions

In summary, we have developed a new class of triple hydrogen-bonding modules, 6-alkynyl-2-amino-3*H*-pyrimidin-4-one derivatives **3** and **7**. In $CDCl_3$, the *N*-alkylated **7** was demonstrated to strongly self-dimerize by ^{1}H NMR experiments, while the *N*-acylated **3** showed much weaker dimerization. DFT calculations and X-ray structure analysis showed that the self-association of **7** is based on the ADD·DAA-type three-point hydrogen-bonding consisted of two kinds of its tautomers. A pyrene fluorophore was connected to the hydrogen-bonding module by Sonogashira reaction to afford **9**, which realized quantitative analyses for the strong associations. The fluorimetric titration of **9** revealed its selective and strong recognition of the module

Table 1. ^{1}H NMR chemical shifts of N*H* protons on the addition of the lipophilic nucleosides to **7**.[a]

Substrates	δ[N*H*(**7**-*endo*)] [ppm]	δ[N*H*(**7**-*exo*)] [ppm]	δ[N*H*(nucleobase)] [ppm]
7[b]	11.22	5.57	
10C[b]			5.04
7·**10C**[b]	13.47	8.24	9.36, 4.96
10G			12.19, 5.68
7·**10G**	11.46	5.94	12.29, 5.46
10U			7.85
7·**10U**	11.19	5.52	8.01
10A			5.45
7·**10A**	11.19	5.55	5.47

[a] Conditions: **7** (1.0×10^{-3} M) and/or **10** (1.0×10^{-3} M) in $CDCl_3$, 22 °C. [b] The spectra were shown in Figure 4.

for a cytosine base. The binding of **9** with cytosine was also predicted to occur in a similar ADD·DAA mode.

Experimental Section

General Remarks: NMR spectra were recorded with a Varian UNITY plus 500 instrument. Chemical shifts were given in ppm relative to TMS (^{1}H, 0.0 ppm) or $CDCl_3$ (^{13}C, 77.0 ppm). IR spectra were obtained with a JASCO FTIR-460plus spectrometer. High and low resolution mass spectra were taken with a JEOL JMS-AX505HAD (EI) or a JEOL AccuTOF JMS T100LC (ESI) instruments. Elemental analyses were performed with a Perkin–Elmer 2400II instrument. Melting points were measured with a Yanaco MP-500D instrument and not corrected. UV/Vis and fluorescence spectra were taken with a JASCO V-560 and a JASCO FP-6500 spectrometer, respectively. Vapor pressure osmometry (VPO) analyses were performed with a Gonotec OSMOMAT 070 instrument. Commercially available materials were used as purchased. Lipophilic nucleotides **10C**,[20] **10G**,[20] **10T**,[21] and **10U**[21] were prepared according to the procedures in literature.

6-Chloro-2-(octanoylamino)-3*H*-pyrimidin-4-one (2): To an ice-cold (0 °C) suspension of 2-amino-4-chloro-6-hydroxypyrimidine (**1**) (4.4 g, 30 mmol) and 4-(dimethylamino)pyridine (DMAP) (8.1 g, 66 mmol) in DMF (60 mL) was added dropwise octanoyl chloride (5.4 g, 33 mmol). The mixture was stirred for 5 h and slowly brought to room temperature. The resulting solution was poured into ice-water (600 mL), and the mixture was stirred for 10 h. The precipitate formed was filtered and recrystallized from AcOEt to afford colorless fibrous crystals of **2** (6.1 g, 77%). M.p. 236–237 °C. ^{1}H NMR (500 MHz, $CDCl_3$): δ = 0.89 (t, J = 7.0 Hz, 3 H), 1.28–1.36 (m, 8 H), 1.69–1.72 (m, 2 H), 2.44 (t, J = 7.5 Hz, 2 H), 6.24 (s, 1 H), 8.50 (br. s, 1 H), 11.91 (br. s, 1 H) ppm. ^{13}C NMR (125 MHz, [D$_6$]DMSO): δ = 13.9, 22.1, 24.2, 28.3, 28.4, 31.1, 36.0, 106.9, 107.0, 151.0, 158.0, 159.8, 176.7 ppm. IR (KBr): $\tilde{\nu}$ = 3092, 2925, 2857, 1667, 1599, 1558 cm^{-1}. EI HRMS: *m*/*z* calcd. for $C_{12}H_{18}ClN_3O_2$ [M$^+$] 271.1088; found 271.1084.

2-(Octanoylamino)-6-(trimethylsilylethynyl)-3*H*-pyrimidin-4-one (3): To a toluene (50 mL) suspension of **2** (0.50 g, 1.8 mmol) and [Pd(PPh$_3$)$_4$] (0.21 g, 0.18 mmol) was added tri-*n*-butyl(trimethylsilylethynyl)stannane (2.1 g, 5.4 mmol) dropwise during 3 h at 80 °C. The mixture was stirred additionally for 2 h at that temperature, cooled to room temperature, and concentrated under a reduced pressure. The resulting residue was purified by silica gel column chromatography (hexane/AcOEt, 9:1) to give **3** (0.50 g, 81%). Further purification can be done by recrystallization from hexane/AcOEt (10:1) to afford colorless fibrous crystals. M.p. 167–174 °C. ^{1}H NMR (500 MHz, $CDCl_3$): δ = 0.24 (s, 9 H), 0.87 (t, J = 7.0 Hz, 3 H), 1.26–1.33 (m, 8 H), 1.64–1.70 (m, 2 H), 2.38 (t, J = 7.5 Hz, 2 H), 6.30 (s, 1 H), 8.14 (br. s, 1 H), 11.81 (br. s, 1 H) ppm. ^{13}C NMR (125 MHz, [D$_6$]DMSO): δ = –0.6, 13.9, 22.1, 24.2, 28.28, 28.35, 31.1, 36.0, 98.3, 101.9, 112.2, 112.4, 146.6, 151.4, 159.8, 176.6 ppm. IR (KBr): $\tilde{\nu}$ = 3154, 2925, 2856, 1647 cm^{-1}. EI HRMS: *m*/*z* calcd. for $C_{17}H_{27}N_3O_2Si$ [M$^+$] 333.1873; found 333.1870.

4-Chloro-6-(methoxymethoxy)-2-(octanoylamino)pyrimidine (4): To an ice-cold (0 °C) suspension of NaH (0.44 g, 11 mmol; commercial 60% dispersion was washed thoroughly with hexane prior to use) and K_2CO_3 (3.0 g, 22 mmol) in DMF (200 mL) was slowly added **2** (2.7 g, 10 mmol). After stirring for 1 h at 0 °C, chloromethyl methyl ether (MOMCl) (0.89 g, 11 mmol) was added to the suspension. The mixture was stirred for an additional 24 h, being slowly warmed from 0 °C to room temperature. The resulting mixture was poured into water (900 mL) and extracted with AcOEt (100 mL × 4). The AcOEt extract was washed with water (200 mL × 2) and brine (100 mL × 2) subsequently, dried with Na_2SO_4, and the solvents evaporated. The residue was purified by silica gel column chromatography (hexane/AcOEt, 9:1) to afford **4** as colorless solid (2.8 g, 87%). M.p. 65–66 °C. ^{1}H NMR (500 MHz, $CDCl_3$): δ = 0.88 (t, J = 7.3 Hz, 3 H), 1.26–1.38 (m, 8 H), 1.69–1.72 (m, 2 H), 2.76 (t, J = 7.5 Hz, 2 H), 3.53 (s, 3 H), 5.52 (s, 2 H), 6.49 (s, 1 H), 7.83 (br. s, 1 H) ppm. ^{13}C NMR (125 MHz, $CDCl_3$): δ = 14.1, 22.6, 24.7, 29.1, 29.2, 31.7, 37.5, 57.8, 93.1, 102.1, 156.4, 161.6, 170.0, 173.6 ppm. IR (KBr): $\tilde{\nu}$ = 3286, 2954, 2927, 2852, 1689, 1563 cm^{-1}. EI MS: *m*/*z* = 315 [M$^+$]. $C_{14}H_{22}ClN_3O_3$ (315.8) calcd. C 53.25, H 6.83, N 13.31; found C 53.20, H 6.83, N 13.30.

4-Chloro-6-(methoxymethoxy)-2-(octylamino)pyrimidine (5): To a THF (10 mL) suspension of $LiAlH_4$ (0.23 g, 6.0 mmol) was added a THF (10 mL) solution of **4** (0.95 g, 3.0 mmol) dropwise at room temperature. The suspension was slowly warmed and refluxed for 1 h. The resulting mixture was cautiously poured into an AcOEt/satd. aq. $NaHCO_3$/ice mixture and was extracted with AcOEt (20 mL × 3). The AcOEt extract was washed with satd. aq. $NaHCO_3$ twice and brine once, dried with Na_2SO_4, and the solvents evaporated. The concentrated residue was purified by silica gel column chromatography (hexane/AcOEt, 10:1) to afford **5** as colorless solid (0.51 g, 56%). M.p. 33–35 °C. ^{1}H NMR (500 MHz, $CDCl_3$): δ = 0.88 (t, J = 7.3 Hz, 3 H), 1.26–1.35 (m, 10 H), 1.53–1.60 (m, 2 H), 3.34–3.39 (m, 2 H), 3.51 (s, 3 H), 5.1–5.5 (br. m, 3 H), 6.07 (s, 1 H) ppm. ^{13}C NMR (125 MHz, $CDCl_3$): δ = 14.2, 22.7, 26.9, 29.28, 29.34, 29.5, 31.8, 41.6, 57.5, 92.2, 95.2, 96.2, 161.2, 161.7, 170.1 ppm. IR (KBr): $\tilde{\nu}$ = 3269, 2926, 2855, 1604, 1579, 1536 cm^{-1}. ESI HRMS: calcd. for $C_{14}H_{24}ClN_3NaO_2$ [M + Na$^+$] 324.1455; found 324.1447.

6-Chloro-2-(octylamino)-3*H*-pyrimidin-4-one (6): To a THF (6 mL) solution of **5** (0.30 g, 1.0 mmol) was added 6 N HCl (6 mL), and the mixture was stirred for 1 h at room temperature. The resulting mixture was diluted with water (30 mL), made alkaline with Na_2CO_3, and extracted with $CHCl_3$ (10 mL × 3). The $CHCl_3$ extract was washed with brine and evaporated to afford **6** as colorless solid (0.26 g, 100%). Further purification was carried out by silica gel column chromatography (CH_2Cl_2/MeOH, 9:1). M.p. 161–162 °C. ^{1}H NMR (500 MHz, $CDCl_3$): δ = 0.88 (t, J = 7.0 Hz, 3 H), 1.25–1.38 (m, 10 H), 1.57–1.63 (m, 2 H), 3.38–3.42 (m, 2 H), 5.72 (s, 1 H), 6.64 (br. s, 1 H), 11.30 (br. s, 1 H) ppm. ^{13}C NMR (125 MHz, $CDCl_3$): δ = 14.2, 22.7, 26.9, 29.2, 29.33, 29.35, 31.9, 41.3, 99.7, 153.8, 162.6, 164.7 ppm. IR (KBr): $\tilde{\nu}$ = 3259, 2953, 2929, 2848, 1671, 1623 cm^{-1}. EI HRMS: calcd. for $C_{12}H_{20}ClN_3O$ [M$^+$] 257.1295; found 257.1297.

2-(Octylamino)-6-(trimethylsilylethynyl)-3*H*-pyrimidin-4-one (7): A xylene (30 mL) solution of **6** (179 mg, 0.69 mmol) and [Pd(PPh$_3$)$_4$] (80 mg, 0.07 mmol) was heated to 120 °C, then to the mixture was added tri-*n*-butyl(trimethylsilylethynyl)stannane (1.34 g, 3.45 mmol) in one portion. The mixture was stirred for 3 h at 120 °C, cooled to room temperature, and diluted with $CHCl_3$ (30 mL). The organic layer was washed with brine twice, dried with Na_2SO_4, and the solvents evaporated. The resulting residue was purified by silica gel column chromatography (CH_2Cl_2/MeOH, 10:1) twice and preparative reverse phase HPLC (COSMOSIL 5SL-II, Nacalai Tesque, Inc.; MeOH/water, 9:1) to afford **7** (48 mg, 22%) as colorless solid. M.p. 34–36 °C. ^{1}H NMR (500 MHz, $CDCl_3$): δ = 0.25 (s, 9 H), 0.88 (t, J = 7.0 Hz, 3 H), 1.28–1.39 (m, 10 H), 1.57–1.62 (m, 2 H), 3.39–3.43 (m, 2 H), 5.86 (s, 1 H), 6.56 (br. s, 1 H), 11.22 (br. s, 1 H) ppm. ^{13}C NMR (125 MHz, $CDCl_3$): δ = –0.34, 14.2, 22.7, 26.9, 29.27, 29.33, 29.34, 31.9, 41.1, 98.3,

102.6, 105.8, 150.9, 154.7, 164.7 ppm. IR (KBr): $\tilde{\nu}$ = 3312, 3145, 2958, 2928, 2857, 1667, 1610 cm^{-1}. EI HRMS: calcd. for $C_{17}H_{29}N_3OSi$ [M^+] 319.2080; found 319.2061.

4-(Methoxymethoxy)-2-(octylamino)-6-(1-pyrenylethynyl)pyrimidine (8): A mixture of **5** (150 mg, 0.50 mmol), 1-ethynylpyrene[22] (120 mg, 0.55 mmol), and $[Pd(PPh_3)_4]$ (58 mg, 0.05 mmol) in Et_3N (10 mL)–THF (10 mL) was stirred at 60 °C for 12 h. The resulting mixture was evaporated and subjected to silica gel column chromatography (benzene to benzene/MeOH, 100:1) to afford **8** as yellow solid (130 mg, 54%). M.p. 110–113 °C. ^{1}H NMR (500 MHz, $CDCl_3$): δ = 0.89 (t, J = 7.0 Hz, 3 H), 1.25–1.41 (m, 10 H), 1.59–1.64 (m, 2 H), 3.44–3.46 (br. m, 2 H), 3.57 (s, 3 H), 5.2 (br. s, 1 H), 5.55 (s, 2 H), 6.47 (s, 1 H), 8.03–8.26 (m, 8 H), 8.65 (d, J = 9.0 Hz, 1 H) ppm. ^{13}C NMR (125 MHz, $CDCl_3$): δ = 14.2, 22.8, 27.1, 29.36, 29.45, 29.7, 31.9, 41.6, 57.5, 90.0, 91.9, 116.1, 124.3, 124.4, 124.6, 125.5, 126.0, 126.1, 126.4, 127.3, 128.4, 128.82, 128.83, 130.3, 131.1, 131.2, 132.1, 132.7, 144.5, 152.2, 162.4 ppm. IR (KBr): $\tilde{\nu}$ = 3243, 2922, 2852, 2213, 1616, 1560 cm^{-1}. ESI HRMS: calcd. for $C_{32}H_{34}N_3O_2$ [M + H^+] 492.2651; found 492,2636.

2-(Octylamino)-6-(1-pyrenylethynyl)-3*H*-pyrimidin-4-one (9): To a THF (2 mL) solution of **8** (49 mg, 0.1 mmol) was added 6 N HCl (2 mL), and the mixture was stirred for 1 h at room temperature. The resulting mixture was diluted with water (10 mL), made alkaline with Na_2CO_3, and extracted with $CHCl_3$ (10 mL × 5). The $CHCl_3$ extract was washed with brine and evaporated to afford **9** as yellow solid (44 mg, 94%). Further purification was carried out by recrystallization from EtOH. M.p. 217–221 °C. ^{1}H NMR (500 MHz, $CDCl_3$): δ = 0.81 (t, J = 7.0 Hz, 3 H), 1.24–1.49 (m, 10 H), 1.69–1.74 (m, 2 H), 3.53–3.57 (m, 2 H), 6.22 (s, 1 H), 6.24 (br. s, 1 H), 8.05–8.27 (m, 8 H), 8.65 (d, J = 9.0 Hz, 1 H), 11.69 (br. s, 1 H) ppm. ^{13}C NMR (125 MHz, [D_6]DMSO): δ = 13.9, 22.1, 26.3, 28.67, 28.70, 29.0, 31.3, 88.9, 94.1, 115.2, 123.3, 123.5, 124.6, 125.0, 126.3, 126.9, 127.2, 128.9, 129.3, 130.0, 130.4, 130.7, 131.65, 131.67, 148.5, 154.9 ppm. IR (KBr): $\tilde{\nu}$ = 3299, 3154, 2923, 2852, 2208, 1661, 1609 cm^{-1}. ESI HRMS: calcd. for $C_{30}H_{30}N_3O$ [M + H^+] 448.2389; found 448.2385.

Evaluation of Association: The dilution, titration, and Job's analyses for **3** and **7** were performed by ^{1}H NMR at 500 MHz in $CDCl_3$, and those for **9** were carried out in $CHCl_3$ using a fluorometer. For the analyses, $CHCl_3$ and $CDCl_3$ were stored over K_2CO_3 and 4-Å molecular sieves (MS), and filtered before use. The binding constants were calculated from the titration curve by using an iterative least-squares curve-fitting method.[23]

Measurement of Fluorescence Lifetime of 9: Fluorescence life time of **9** was measured by time correlation, a single-photon counting methodology using a Horiba NAES-550 nanosecond fluorometer. The excitation wavelength was 400 nm and emissions were detected in the range of 380–500 nm. These measurements were performed at concentrations of 1.0×10^{-5} M under Ar. The fluorescence decay profile was analyzed on the basis of the following equation: $F(t) = F_0 \exp(-t/\tau)$.

Computational Method: Quantum chemical calculations were carried out with the Gaussian 98 program. The evaluation of the total electronic energies was performed by the use of DFT(B3LYP) method and 6-31G(d,p) basis sets.

X-ray Structure Studies: The single crystals of compound **7** were obtained by slow evaporation from a $CDCl_3$ solution as very wet crystals. Structure analysis at room temperature showed disordered terminal trimethylsilyl and octyl groups. At –50 °C, the disorder of the trimethylsilyl group was solved whereas the octyl group was still disordered. Crystal data: $C_{17}H_{29}N_3OSi$, M_w = 319.52, orthorhombic, *Pnna*, Z = 8, a = 27.907(2), b = 17.7080(7), c = 8.3452(4) Å, $D_{calcd.}$ = 1.029 g/cm^3, 20154 reflections were collected, 4255 unique (R_{int} = 0.078), 1357 observed [$I > 2\sigma(I)$], 198 parameters, R_1 = 0.136, wR_2 = 0.329. GOF = 1.23, refinement on F^2. The data were collected with a Rigaku Raxis-CS imaging plate diffractometer with a graphite-monochromated Mo-K_α radiation (40 kV, 100 mA) to a maximum 2θ value of 55° at –50 °C under cold N_2 gas flow. The camera length was set to be 143.5 mm from the crystal. A total of 56 ($\Delta\varphi$ = 3°) images were measured using an oscillation technique. An absorption correction was not applied and a correction for secondary extinction was applied. The structures were solved by the direct method (*SIR92*[24]) and refined by least-squares calculations using the *teXsan* program package.[25] All non-hydrogen atoms were refined anisotropically except for the disordered terminal two carbon atoms of the octyl group. These carbon atoms were refined on the assumption that they are disordered in two conformations with 50% occupancy. The hydrogen atoms were located on the calculated positions and not refined.

CCDC-259922 contains the supplementary crystallographic data for this paper. These data can be obtained free of charge from The Cambridge Crystallographic Data Centre via www.ccdc.cam.ac.uk/data_request/cif.

Supporting Information: Figures S1–S8, ^{1}H NMR spectra for **2**–**9**, the details of the calculations for the structures shown in Schemes 3–5, cytosine, guanine, and **7a**·cytosine and **7a**,**b**,**f**·guanine complexes.

Acknowledgments

The authors are grateful to Professor Kazuhiko Mizuno (Osaka Prefecture University) for fluorescence lifetime measurements and Professor Atsuhiro Osuka (Kyoto University) and Professor Hiroyuki Furuta (Kyushu University) for vapor pressure osmometry analyses.

[1] For a review for hydrogen-bonding modules, see: S. C. Zimmerman, P. S. Corbin, *Struct. Bonding (Berlin)* **2000**, *96*, 63–94.

[2] For recent reviews for assembling by hydrogen-bonding, see: J. R. Fredericks, A. D. Hamilton, in: *Comprehensive Supramolecular Chemistry* (Eds.: J. L. Atwood, J. E. D. Davies, D. D. MacNicol, F. Vögtle, J.-M. Lehn, J.-P. Sauvage, M. W. Hosseini), Elsevier, Oxford **1996**, vol. 9, pp. 565–594; L. J. Prins, D. N. Reinhoudt, P. Timmerman, *Angew. Chem. Int. Ed.* **2001**, *40*, 2382–2426; L. Brunsveld, B. J. B. Folmer, E. W. Meijer, R. P. Sijbesma, *Chem. Rev.* **2001**, *101*, 4071–4097; D. C. Sherrington, K. A. Taskinen, *Chem. Soc. Rev.* **2001**, *30*, 83–93; M. M. Conn, J. Rebek Jr., *Chem. Rev.* **1997**, *97*, 1647–1668; D. Philp, J. F. Stoddart, *Angew. Chem. Int. Ed. Engl.* **1996**, *35*, 1154–1196; D. S. Lawrence, T. Jiang, M. Levett, *Chem. Rev.* **1995**, *95*, 2229–2260; J.-M. Lehn, *Angew. Chem. Int. Ed. Engl.* **1990**, *29*, 1304–1319.

[3] For recent works for complementary hydrogen-bonding modules, see: G. B. W. L. Ligthart, H. Ohkawa, R. P. Sijbesma, E. W. Meijer, *J. Am. Chem. Soc.* **2005**, *127*, 810–811; A. T. ten Cate, H. Kooijman, A. L. Spek, R. P. Sijbesma, E. W. Meijer, *J. Am. Chem. Soc.* **2004**, *126*, 3801–3808; J. H. K. K. Hirschberg, R. A. Koevoets, R. P. Sijbesma, E. W. Meijer, *Chem. Eur. J.* **2003**, *9*, 4222–4231; R. P. Sijbesma, E. W. Meijer, *Chem. Commun.* **2003**, 5–16; A. El-ghayoury, A. P. H. J. Schenning, P. A. van Hal, J. K. J. van Duren, R. A. J. Janssen, E. W. Meijer, *Angew. Chem. Int. Ed.* **2001**, *40*, 3660–3663; S. H. M. Söntjens, R. P. Sijbesma, M. H. P. van Genderen, E. W. Meijer, *J. Am. Chem. Soc.* **2000**, *122*, 7487–7493; F. H. Beijer, R. P. Sijbesma, H. Kooijman, A. L. Spek, E. W. Meijer, *J. Am. Chem. Soc.* **1998**, *120*, 6761–6769; P. S. Corbin, S. C.

Zimmerman, P. A. Thiessen, N. A. Hawryluk, T. J. Murray, *J. Am. Chem. Soc.* **2001**, *123*, 10475–10488; P. S. Corbin, S. C. Zimmerman, *J. Am. Chem. Soc.* **1998**, *120*, 9710–9711; S. Hikishima, N. Minakawa, K. Kuramoto, Y. Fujisawa, M. Ogawa, A. Matsuda, *Angew. Chem. Int. Ed.* **2005**, *44*, 596–598; J. T. Han, D. H. Lee, C. Y. Ryu, K. Cho, *J. Am. Chem. Soc.* **2004**, *126*, 4796–4797; S. Zou, Z. Zhang, R. Förch, W. Knoll, H. Schönherr, G. J. Vancso, *Langmuir* **2003**, *19*, 8618–8621; K. Yamauchi, J. R. Lizotte, T. E. Long, *Macromolecules* **2003**, *36*, 1083–1088; K. Yamauchi, J. R. Lizotte, D. M. Hercules, M. J. Vergne, T. E. Long, *J. Am. Chem. Soc.* **2002**, *124*, 8599–8604; X. Zhao, X.-Z. Wang, X.-K. Jiang, Y.-Q. Chen, Z.-T. Li, G.-J. Chen, *J. Am. Chem. Soc.* **2003**, *125*, 15128–15139.

[4] A. Kaito, M. Hatano, T. Ueda, S. Shibuya, *Bull. Chem. Soc. Jpn.* **1980**, *53*, 3073–3078 and references cited therein.

[5] P. Bühlmann, W. Simon, *Tetrahedron* **1993**, *49*, 7627–7636; P. Bühlmann, M. Badertscher, W. Simon, *Tetrahedron* **1993**, *49*, 595–598.

[6] For three-point self-assembly of isocytosines, see: a) L. M. Toledo, K. Musa, J. W. Lauher, F. W. Fowler, *Chem. Mater.* **1995**, *7*, 1639–1647; b) B. D. Sharma, J. F. McConnell, *Acta Crystallogr.* **1965**, *19*, 797–806.

[7] For AD·DA-type self-assembly of isocytosines, see: R. Custelcean, L. Craciun, *Tetrahedron* **2000**, *56*, 5067–5075; P. R. Lowe, C. H. Schwalbe, *Acta Crystallogr. Sect. C* **1987**, *43*, 330–333. See also ref.[6a].

[8] R. J. Griffin, C. H. Schwalbe, M. F. G. Stevens, K. P. J. Wong, *J. Chem. Soc., Perkin Trans. 1* **1985**, 2267–2276.

[9] R.-F. Liao, J. W. Lauher, F. W. Fowler, *Tetrahedron* **1996**, *52*, 3153–3162.

[10] A. Schmidt, M. K. Kindermann, *Chem. Lett.* **2001**, 348–349; A. Schmidt, N. Kobakhidze, M. K. Kindermann, *J. Chem. Soc., Perkin Trans. 1* **2002**, 982–990.

[11] H. Vranken, J. Smets, G. Maes, L. Lapinski, M. J. Nowak, L. Adamowicz, *Spectrochim. Acta A* **1994**, *50*, 875–890 and references cited therein.

[12] J. S. Kwiatkowski, J. Leszczynski, *Int. J. Quant. Chem.* **1997**, *61*, 453–465.

[13] T.-K. Ha, H. J. Keller, R. Gunde, H. H. Gunthard, *J. Mol. Struct.* **1996**, *376*, 375–397; C. Roberts, R. Bandaru, C. Switzer, *J. Am. Chem. Soc.* **1997**, *119*, 4640–4649.

[14] Inhibition of cross-association by intramolecular hydrogen bonding was reported, see: S. Brammer, U. Lüning, C. Kühl, *Eur. J. Org. Chem.* **2002**, 4054–4062; See also: J. R. Quinn, S. C. Zimmerman, *Org. Lett.* **2004**, *6*, 1649–1652.

[15] W. L. Jorgensen, J. Pranata, *J. Am. Chem. Soc.* **1990**, *112*, 2008–2010; J. Pranata, S. G. Wierschke, W. L. Jorgensen, *J. Am. Chem. Soc.* **1991**, *113*, 2810–2819; T. J. Murray, S. C. Zimmerman, *J. Am. Chem. Soc.* **1992**, *114*, 4010–4011.

[16] M. Inouye, K. Takahashi, H. Nakazumi, *J. Am. Chem. Soc.* **1999**, *121*, 341–345; C.-Y. Huang, L. A. Cabell, *J. Am. Chem. Soc.* **1994**, *116*, 2778–2792; P. Murray-Rust, J. P. Glusker, *J. Am. Chem. Soc.* **1984**, *106*, 1018–1025; S. J. Weiner, P. A. Kollman, D. A. Case, U. C. Singh, C. Ghio, G. Alagona, S. Profeta Jr., P. Weiner, *J. Am. Chem. Soc.* **1984**, *106*, 765–784.

[17] J. Šponer, P. Hobza, *J. Phys. Chem. A* **2000**, *104*, 4592–4597; N. U. Zhanpeisov, J. Šponer, J. Leszczynski, *J. Phys. Chem. A* **1998**, *102*, 10374–10379; N. U. Zhanpeisov, J. Leszczynski, *J. Phys. Chem. B* **1998**, *102*, 9109–9118; N. U. Zhanpeisov, J. Leszczynski, *Int. J. Quant. Chem.* **1998**, *69*, 37–47.

[18] J. Sartorius, H.-J. Schneider, *Chem. Eur. J.* **1996**, *2*, 1446–1452; P. Carmona, M. Molina, A. Lasagabaster, R. Escobar, A. B. Altabef, *J. Phys. Chem.* **1993**, *97*, 9519–9524; Y. Kyogoku, R. C. Lord, A. Rich, *Biochim. Biophys. Acta* **1969**, *179*, 10–17.

[19] J. L. Sessler, M. Sathiosatham, C. T. Brown, T. A. Rhodes, G. Wiederrecht, *J. Am. Chem. Soc.* **2001**, *123*, 3655–3660; J. L. Sessler, B. Wang, A. Harriman, *J. Am. Chem. Soc.* **1995**, *117*, 704–714.

[20] K. K. Ogilvie, A. L. Schifman, C. L. Penny, *Can. J. Chem.* **1979**, *57*, 2230–2238.

[21] K. K. Ogilvie, S. L. Beaucage, A. L. Schifman, N. Y. Theriault, K. L. Sadana, *Can. J. Chem.* **1978**, *56*, 2768–2780.

[22] M. Hissler, A. Harriman, A. Khatyr, R. Ziessel, *Chem. Eur. J.* **1999**, *5*, 3366–3381.

[23] K. A. Connors, *Binding Constants*, John Wiley & Sons, New York, **1987**.

[24] A. Altomare, G. Cascarano, C. Giacovazzo, A. Guagliardi, M. C. Burla, G. Polidori, M. Camalli, *J. Appl. Crystallogr.* **1994**, *27*, 435.

[25] Single Crystal Structure Analysis Software. Version 1.11: Molecular Structure Corporation, 3200 Research Forest Drive, The Woodlands, TX 77381, USA, **2000**.

Received: January 07, 2005
Published Online: June 2, 2005

